Examining Cross Frequency Interference Effects in Multi-Frequency GNSS Receivers

Sherman Lo, Yu Hsuan Chen, Nicolas San Miguel, Todd Walter, *Stanford University*
Dennis Akos, *University of Colorado Boulder*

Biographies

Sherman Lo is a senior research engineer at the Stanford GPS Laboratory and the executive director of the Stanford Center for Position Navigation and Time. He received his Ph.D. in Aeronautics and Astronautics from Stanford University in 2002. He has and continues to work on navigation robustness and safety, often supporting the FAA. He has conducted research on Loran, alternative navigation, SBAS, ARAIM, GNSS for railways and automobile. He also works on spoof and interference mitigation for navigation. He has published over 100 research papers and articles. He was awarded the ION Early Achievement Award.

Yu-Hsuan Chen is a research engineer at the Stanford GPS Laboratory. He received his Ph.D. in Electrical Engineering from National Cheng Kung University, Taiwan in 2011.

Nicolas San Miguel is a graduate student in the Stanford GPS Laboratory in Aeronautics and Astronautics at Stanford University. He received his B.S. in Aerospace Engineering from the Georgia Institute of Technology in 2021.

Todd Walter is professor of research in the Department of Aeronautics & Astronautics. He directs at the Stanford GPS Laboratory. He received his Ph.D. in Applied Physics from Stanford University.

Dennis Akos completed the Ph.D. degree in Electrical Engineering at Ohio University within the Avionics Engineering Center. He is a faculty member with the Aerospace Engineering Sciences Department at the University of Colorado, Boulder

Abstract

Radiofrequency interference (RFI) can have many effects on GNSS receivers. One effect that is less commonly discussed is how RFI on one GNSS frequency band may affect a separate frequency band due to the design of its user equipment (antenna, receiver). It is useful to examine these effects to better understand actual receiver vulnerabilities. It helps with developing specifications and guidelines to limit such vulnerabilities. Furthermore, understanding and limiting these effects can help more effectively develop receiver based detect spoofing and jamming.

This paper examines cross frequency effects through empirical testing of several types of GNSS antennas and receivers. Equipment ranging from consumer off the shelf (COTS) to high end survey grade were tested in an anechoic chamber with re-radiated GNSS and interference signals. The system response is analyzed by looking at spectrum, automatic gain control (AGC), and carrier to noise ratio (C/No) results on multiple frequency band when there is RFI on one frequency band. The antennas tested showed different behavior with the same RFI across frequency bands. One antenna had little cross frequency effects while the other showed some noticeable effects on one band from interference on another. Different receivers also showed different responses across frequency bands with the same RFI. For example, we tested three models of dual frequency GNSS smartphone tested. One model could not utilize L5 when there was interference on L1 while other smartphones did not show this effect.

This paper highlights different cross frequency effects that occur with RFI with different empirical tests. It demonstrates the importance of understanding implementation and actual performance and not just assuming each frequency band will operate independently.

1. INTRODUCTION

Multi-frequency GNSS receiver systems are increasingly commonplace. They are now found in numerous consumer mass market devices including smartphones and smartwatches. Importantly, they are being adopted for safety and economically critical applications. This is happening in aviation with the development of dual frequency multi-constellation (DFMC) standards for satellite-based augmentation systems as well as advanced receiver autonomous integrity monitoring (ARAIM). A major reason for adopting multi-frequency rather than L1 only receivers is for their benefits in improving positioning performance. Another motivation for using multi-frequency receiver is increased resiliency to radiofrequency interference (RFI) due to frequency diversity. This paper examines one of the tenets supporting this benefit – that the different frequency channels are independent with regards to RFI.

This paper empirically examines the effect of RFI on one GNSS frequency band on another frequency band. This cross-frequency band effects may occur due to different factors such as receiver or antenna design. It is useful to examine these effects for two main reasons. The first is to better understand user receiver vulnerabilities. If RFI on one frequency affects the receiver processing of another, this would make it less than resilient than advertised or anticipated. So we want to know the actual RFI vulnerabilities of our multi-frequency system. Second, knowing the causes of cross frequency effects can help us develop specifications to limit such vulnerabilities. And if we understand and limit these effects, we can more confidently use our receiver to detect spoofing and jamming. For example, we can more confidently compare results across frequencies in determining problems.

The cross-frequency study is conducted by testing of several types of GNSS antennas and receivers. GNSS antennas and receivers from mass market consumer off the shelf (COTS), higher end COTs and survey grade were tested in an anechoic chamber with re-radiated GNSS and interference signals. The system response is analyzed by looking at spectrum, automatic gain control (AGC), and carrier to noise ratio (C/No) results on multiple frequency band when there is RFI on one frequency band. The results show varying effects from none to significant. The tests are meant to illustrate some potential responses of our multi-frequency GNSS units to interference on one frequency. The purpose of this paper is to show some example effects rather than to definitively account for the effects. It is meant to draw awareness and solicit feedback about the different cross frequency effects on GNSS units.

2. BACKGROUND

GNSS user equipment from the antenna to the receiver can be very complicated systems. They can respond in surprising and unexpected, at least to the users, ways to unusual, though not necessarily rare, events such as jamming. For example, maritime receivers in GNSS jamming trials conducted by the General Lighthouse Association (GLA) in 2006 had several receivers provide greatly erroneous positions with some providing little indication of an issue with or loss of GNSS (Grant et al, 2009). Today, receivers can be even more complicated as they can employ more hardware components and more sophisticated processing. They are being hardened with increasingly sophisticated processing to mitigate issues like interference or improve sensitivity. Since the processing is often proprietary or not generally available, it is not clear if such processing may have unintended effects.

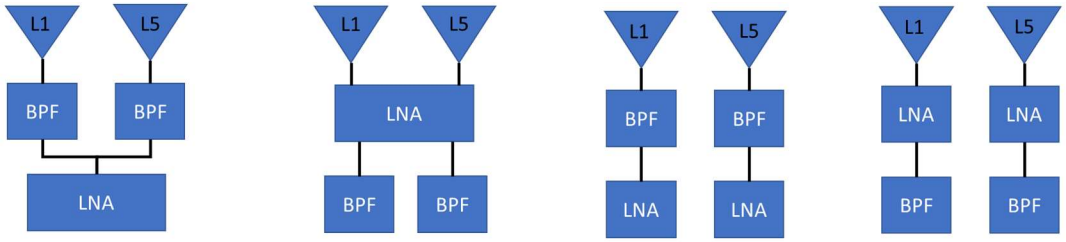

BPF before Common LNA
Reduces out of band interference effects but with higher noise
Jamming one frequency may affect another by saturating LNA

BPF after Common LNA
Common implementation with lower noise
Jamming one band may affect another by saturating LNA

Separate BPF then LNA
Two isolated channel but more expensive

Separate LNA then BPF
Two isolated channel but more expensive
Lower noise

Figure 1. Generic Simplified LNA/BPF Antenna Layouts Options

The choices made by the GNSS antenna or receiver designer is influenced by many different factors. Factors such as cost or noise figure can result in design choices that could impacts on the cross-frequency performance. Figure 1 shows some simple block diagrams of how a dual frequency antenna with low noise amplifier (LNA) and band pass filters (BPF) may be designed. A design with two completely independent radio frequency (RF) chains may be best for performance but induces more cost as no components are shared. Conversely, a design that shares components such as LNA to reduce cost may suffer in terms of performance as well as have cross frequency effects. Another choice is relative placement of the LNA and BPF. For example, having LNA immediately after the antenna element reduces noise but this design may be more susceptible to interference. Given the creativity and diversity in GNSS hardware, it would not be surprising to see lots of different implementation of a multi-frequency GNSS antenna or receiver. The diversity can be seen in the specification sheets of the two mass market antennas tested - see Figure 4 and Figure 5. Hence, we wanted to look at some examples of different classes of hardware to see how these designs, given their choices, may affect cross frequency effects and hence resiliency.

3. EXPERIMENTAL SETUP

Test Set Up

The testing was conducted in an anechoic chamber using re-radiated live GNSS signal capture from the nearby roof and interference generated by a software defined radio (SDR), each transmitted into the chamber from separate antennas. The chamber is roughly 35.5 x 30 x 27 inches and is shown in Figure 2. The genuine GNSS signal is capture by a roof-top Trimble Zephyr 2 multi-frequency antenna and sent to the helical antenna (long antenna in the middle of picture in Figure 2) to be re-radiated inside the chamber. The Zephyr is located at the top of the Stanford Department of Aeronautics & Astronautics in reasonably noise free and low multipath conditions. However, there is a nearby VORTAC (VOR plus TACAN) station in Woodside (OSI) which broadcasts on 1173 MHz in the L5 band. There are a few other distance measuring equipment (DME) stations that are a little further away that transmit near L5 – Oakland at 1202 MHz and Sausalito at 1196 MHz – see Table 3 in (Lo et al, 2015). The interference signal is generated by a SDR and transmitted from the smaller (marine) helical antenna. The transmitted power is controlled by a variable attenuator. The interference helical antenna is about 46 cm from the target area. Based on the SDR output power (10 deciBels (dB) relative to a milliWatt (dBm)) and the LNA gain (maximum of 36 dB), the nominal transmitted power is estimated to vary from 13 to 46 dBm. This results in a maximum received interference power is roughly 19 dBm. This may be about 8 dB too high as our spectrum analyzer measured only 1.7 dBm coming from the USRP. The equipment under test, typically an antenna, is placed at center of the chamber, directly under the re-radiating helical antenna. The antenna under test is connected to a receiver which can reside outside the chamber. The chamber has antenna ports that connect the interior to the exterior. However, smartphones under test are tested inside the chamber. The interference tests typically last about five minutes with the first 60 seconds without interference and gradually increasing interference.

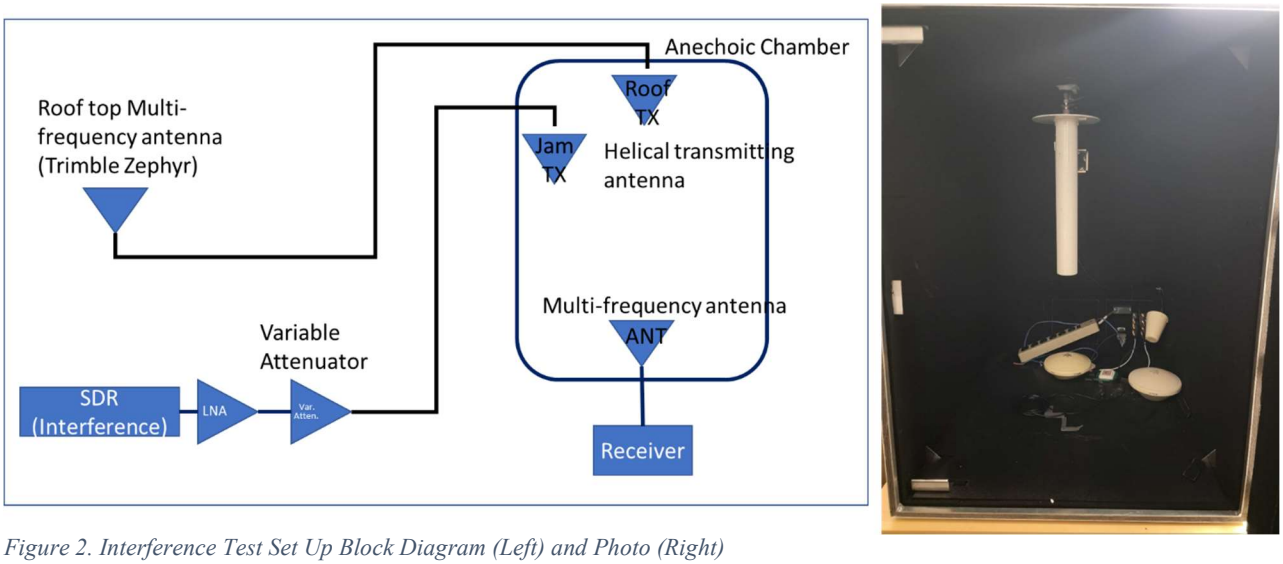

Figure 2. Interference Test Set Up Block Diagram (Left) and Photo (Right)

Several interference signals were tested. Both additive white gaussian noise (AWGN) and continuous wave (CW) interference were used with their parameters given in Table 1. The continuous wave interference is centered at L1 (1575.42 MHz) with tones offset by ± 0.5 MHz. The AWGN is center at L1 (1575.42 MHz) with a bandwidth of 40 MHz. They are both transmitted with the same power profile. The power level of interference was gradually increased in steps as shown in Figure 3. The jamming starts after 60 seconds with a power level of 13 dBm at the antenna, stepping up by 3 dB every 5 seconds. It ends 55 seconds later (at 115 seconds after start) at 46 dBm. The jamming is held at 46 dBm until 210 seconds after start.

Table 1. Interference Signals Tested

Interference Signal	Center Frequency (MHz)	Bandwidth (MHz)
Continuous Wave	1574.92 & 1575.92	2 tones
Additive White Gaussian Noise	1575.42	40 MHz

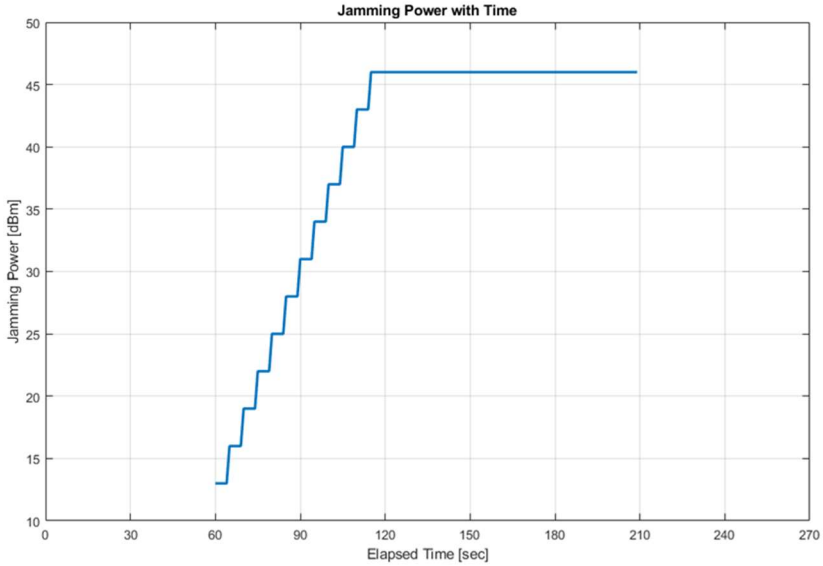

Figure 3. Jammer Transmitted Power Profile of Interference Test

Equipment Under Test

Several different antenna and receivers were used. We choose three antennas representing different classes of equipment. We used: 1) high precision Trimble Zephyr 2, 2) original equipment manufacturer (OEM) L1/L5 antenna (ArduSimple simpleANT2B-OEM ~ $70) and 3) consumer level antenna u-blox L1/L5 antenna (ANN-MB1 ~$35). Figure 4 and Figure 5 show the simplified block diagram for the ArduSimple and u-blox antennas, respectively. Both antenna RF chains feature two sets of BPF, such as a surface acoustic wave (SAW) filter, followed by an LNA. In the case of the u-blox, the second LNA is one that is shared between both frequencies. The Trimble Zephyr used is a survey grade antenna with a four-point antenna feed and is more expensive than the other two antenna. We also tested different types of receivers from a COTS u-blox L1/L5 (F9T-10B), Septentrio Mosaic-X5, and Trimble BX940. As the most common receivers are smartphones, we also tested several multi-frequency GNSS smartphones with their GNSS module indicated in (): Xiaomi Mi 8 International version (Broadcomm BCM47755), Samsung S20 5G (Snapdragon 865 SOC GNSS), Samsung S21 Ultra 5G (Snapdragon 888 SOC GNSS).

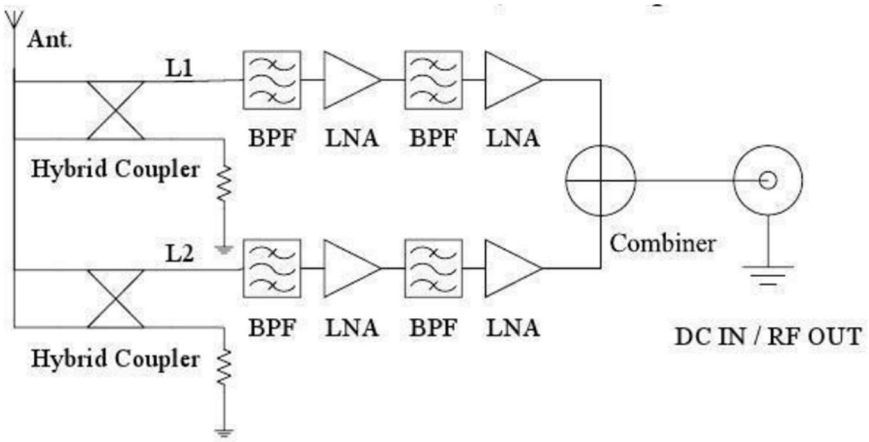

Figure 4. Simplified Block Diagram of ArduSimple ANT2B Antenna from Datasheet (ArduSimple ANT2B Datasheet)

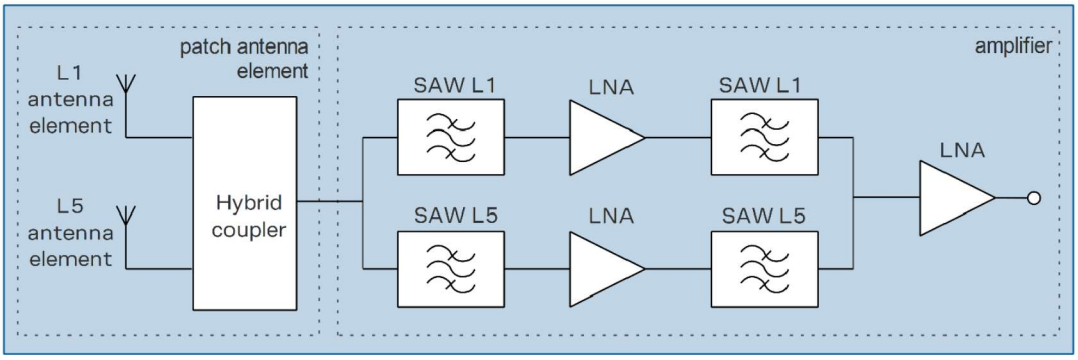

Figure 5. Simplified Block Diagram of u-blox ANN-MB1-00 Antenna from Datasheet (u-blox ANN-MB1-00 Datasheet)

4. TEST RESULTS AND OBSERVATIONS

The paper focuses on a few select tests on antenna and receivers where we introduce jamming on L1 only. We conducted other tests as there are many possible combinations factors to vary such as jamming frequency, jamming types, equipment set up, etc. Again, our goal is to understand potential issues rather than fully comprehensive (which would be difficult given all the different possibilities). To simplify our task, we vary different factors (antenna and receivers shown here) while keeping other factors the constant.

There are many metrics that we can look at. We focus primarily on automatic gain control (AGC) level and carrier to noise ratio (C/No) levels, both of which are measured within a receiver. AGC is a useful measure as it is related the power coming into the receiver (Bastide, et. al, 2003). The receiver AGC adapts its gain such that the incoming energy (signal plus noise) is reasonably constant. This allows for efficient use of its analog to digital conversion (ADC). Hence, AGC gain level is inversely proportional to incoming energy. In GNSS, the incoming energy is dominated by noise, the AGC gain level is effectively a measure of noise power from the receiver. A drawback with AGC is that it is not available in every receiver. Also, the levels and quantization are receiver dependent. C/No is a measure of tracked signal power relative to noise level. This is a common measure available in nearly all receivers and there are a few standard ways of calculating C/No. The drawback is that C/No requires receiver processing and hence is dependent on receiver implementation. Other factors that we examine is spectrum and positioning (in the case of receiver performance).

Antenna Test

Three antennas (ArduSimple, u-blox, Trimble) were tested separately under nearly the same conditions with the only difference being the GNSS signal since it was a live signal. For the antenna test results shown, a Septentrio Mosiac-X5 was used as the

common receiver to provide AGC, C/No and spectrum outputs. The receiver is a reasonable choice for several reasons. First, it provides AGC gain levels. AGC level is not provided by the Trimble and provided at a lower resolution on the u-blox. It can provide spectrum performance plots to see interference (the Trimble BX940 can also do similar but we did not capture that information). It should be noted that the spectrum results are generated after applying the AGC. To see absolute spectral energy, we rescaled the plots with the AGC values to normalize them to the same level over time.

Continuous Wave Interference (CWI)

CW interference results are first shown as these have the most variation. First, we examine AGC and C/No results for each receiver. Figure 6 shows the AGC results for the Trimble antenna on multiple bands (L1, L2, etc.). It shows that the AGC gain immediately drops on L1 related bands (L1, E1, B1 and GLONASS L1) to -10 dB, the lowest AGC gain reported by the Septentrio. This indicates that the base level of interference, after going through the antenna, is enough to exceed the maximum input for the receiver, even with filtering from the BPF. GLONASS L1 is not as affected by interference as the CW is ~ 25 MHz from its frequencies. Hence, that band experiences less interference power. The GLONASS L1 AGC thus is not immediately at the lowest value and exhibits a step decrease with each step increase in interference power. The L2 and L5 show no degradation in the AGC gain. More surprisingly, the L2 and L5 bands actually increase in gain which implies a reduction of input power. It steps up, presumable with each step increase in jamming. The final change in AGC gain is an increase of about 4 dB from the initial value and occurs about 50 seconds after the onset of jamming. This is roughly when the jamming power is at a maximum. AGC gain increases should mean decreases in incoming power (signal and noise). Note that the genuine transmission is not changing. This is likely due to a phenomenon in radio design called weak or small signal suppression (also hard limiter suppression) whereby if there are multiple signals entering, the weaker signal tends to proportionally weakened more due to bandpass hard limiter effects (Amoroso, 2003). This effect generally occurs when the relevant amplifier is driven to saturation. Amoroso indicates a typical 6 dB suppression when the interference is much stronger but can be smaller or larger depending on design. It can be smaller when the interference is lower and this is suggested by the gradual increase in L2 and L5 AGC as the interference power is increased. This has been a topic of interest for quite some time (Davenport, 1953). Note that the AGC gain level for these signals increase together and by roughly the same amount. Figure 7 show the C/No on L1 and L2 (Right). The C/No quickly goes away on L1 with the onset and increase of jamming power as one would expect. There seems to be little to no effect on L2 as one would desire from a multi-frequency receiver.

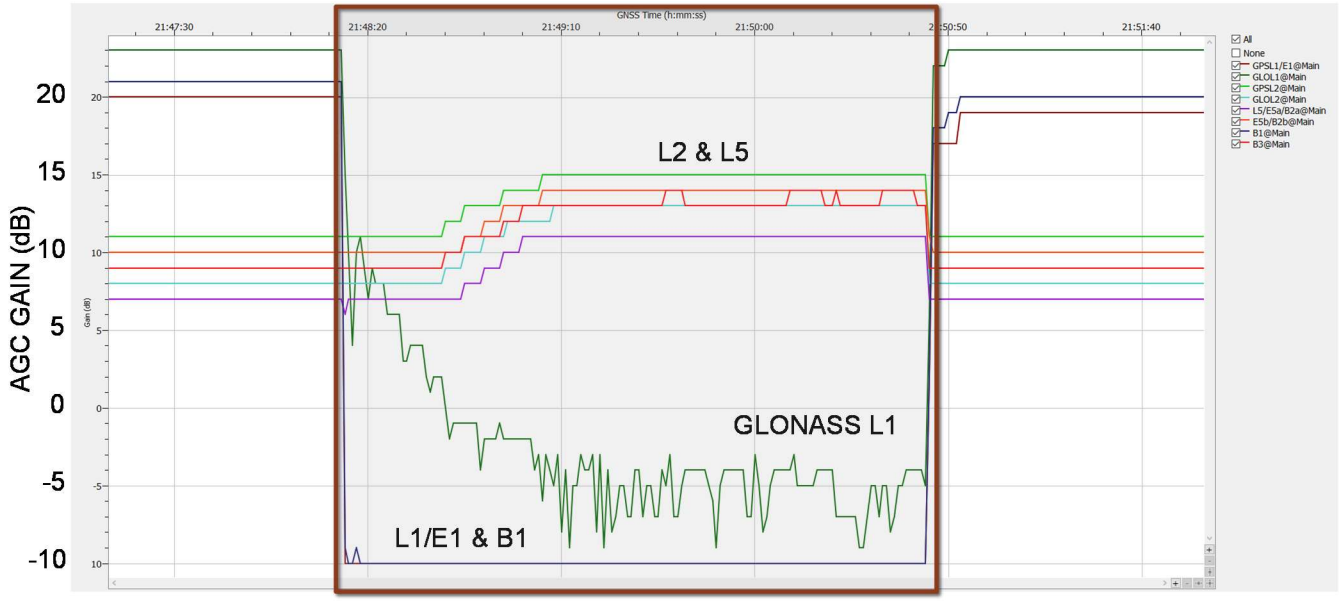

Figure 6. AGC Gain (from Septentrio X5) through Trimble Zephyr Antenna during CW Interference Test (Jamming Period highlighted in box)

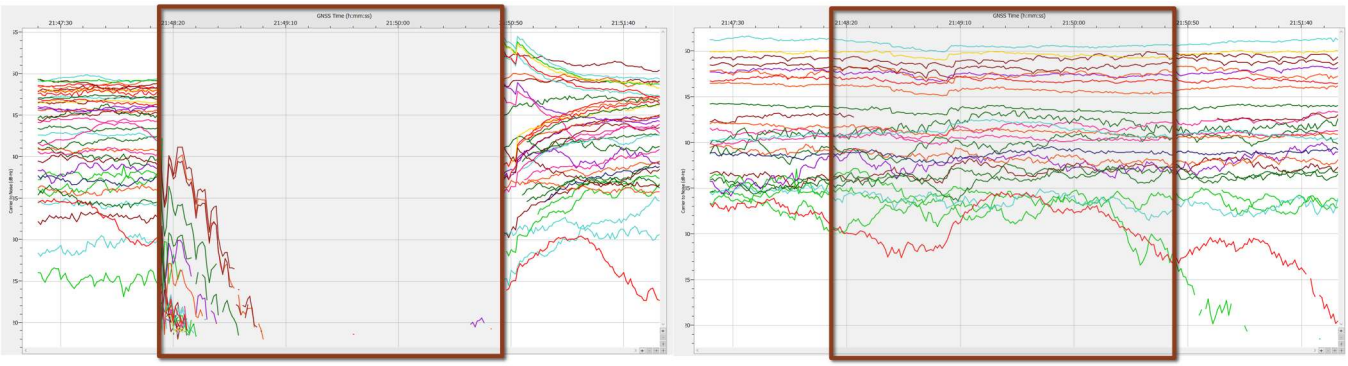

Figure 7. C/No on L1 (Left) and L2 (Right) (from Septentrio X5) through Trimble Zephyr Antenna during CW Interference Test (Jamming Period highlighted in box)

The AGC gain from the Septentrio with u-blox antenna, as seen in Figure 8, demonstrated similar behavior to that seen with the Trimble antenna. The L1 AGC levels behave as expected with an initial large drop with the onset of jamming. It takes a little more time than the Trimble (a few jamming increase steps) to reach the minimum AGC gain level of the Septentrio. The L2 and L5 AGC gain also starts to increase about 45 seconds after the onset of jamming and increases with increasing the jamming power. The maximum AGC gain change is about 10 dB. E5b (1207.14 MHz) and L5/E5a (1176.45 MHz) AGC gain increase by a similar amount. GLONASS L2 (~ 1245 MHz) and Beidou B3 (1268.52 MHz) AGC gain increase by a similar but smaller amount than the L5/E5. The gain tops out at 58 dB. As discussed previously, this is likely due to weak signal suppression and its behavior suggests that it is caused by this phenomenon. We do find different behavior when we examine the C/No, shown in Figure 9. The L1 C/No behaves as expected with jamming quickly causing loss of signal tracking. The L2 C/No is surprising as, unlike in the case with the Trimble antenna, there is a noticeable effect corresponding to the increase L2 AGC gain. The L2 C/No decreases simultaneously across many satellites by a few dB at the same time as the L2 AGC gain starts to increase. This shows some cross-frequency effects from use of the u-blox antenna that we did not see when using the Trimble antenna. That is, there seems to be some degradation of the L2 signal from the L1 interference. This may be due to another saturation effect. Out of band harmonics can be generated if a radio frequency front end component such as a mixer or amplifier is driven with too much power (saturation) which results in nonlinearities and additional spectral products. So driving the L1 signal LNA to saturation may produce additional L2 noise. The instantaneous (rather than gradual) nature of the C/No decrease suggests a nonlinear process such as saturation induced spectral products.

Figure 8. AGC Gain (from Septentrio X5) through u-blox ANN-MB1-00 Antenna during CW Interference Test (Jamming Period highlighted in box)

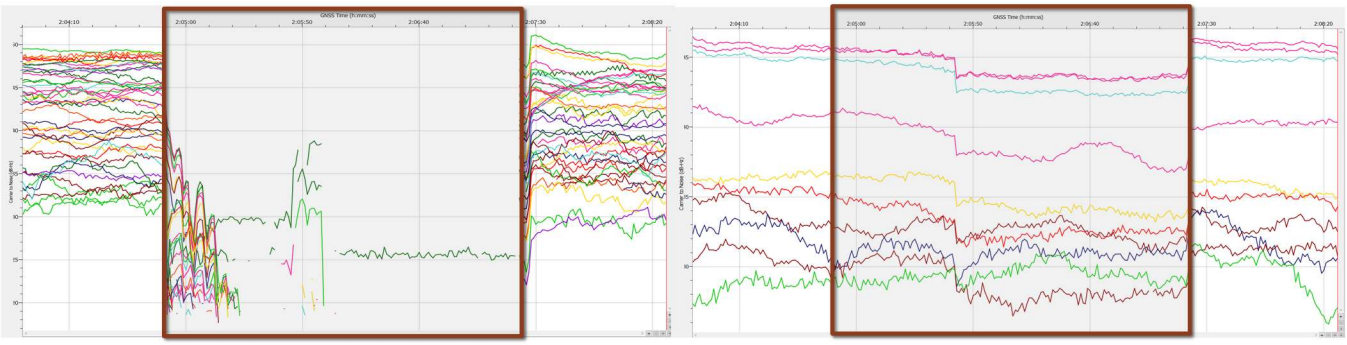

Figure 9. C/No on L1 (Left) and L2 (Right) (from Septentrio X5) through u-blox ANN-MB1-00 Antenna during CW Interference Test (Jamming Period highlighted in box)

The AGC results from the Septentrio receiver when using the ArduSimple antenna, shown in Figure 10, presents a different behavior from the other antenna. The L1 band behaves as expected with the jamming resulting a pretty immediate and rapid drop in AGC gain. The initial onset of jamming reduces the gain by a little over 40 dB and the next two jamming power increase steps reduce the AGC gain to the minimum gain level. More interesting is that the L2 and L5 AGC gain drops by 20 dB during jamming. This does not occur immediately but rather about 45 seconds after the start of jamming with the full 20 dB drop. The instantaneous change (drop) in L2/L5 AGC levels is different from what is seen on the other antenna suggesting a different cause. It could be increase in L2/L5 noise due to nonlinear products due to saturation of RF components. During this period, the changes in AGC gain are different but result in the L5/E5a (1176.45 MHz) and E5b (1207.14 MHz) AGC gain being at roughly the same level. The GPS L2 (1227.6 MHz), GLONASS L2 (~ 1245 MHz) and Beidou B3 (1268.52 MHz) also have different changes in AGC level and are at the same (but different from L5/E5a/E5b) AGC gain level. There is a greater frequency band dependency of the AGC level than with the AGC results from the Trimble and perhaps the u-blox. Both the instantaneous drop and frequency band dependency suggesting another phenomenon at work than just what was seen with the Trimble antenna.

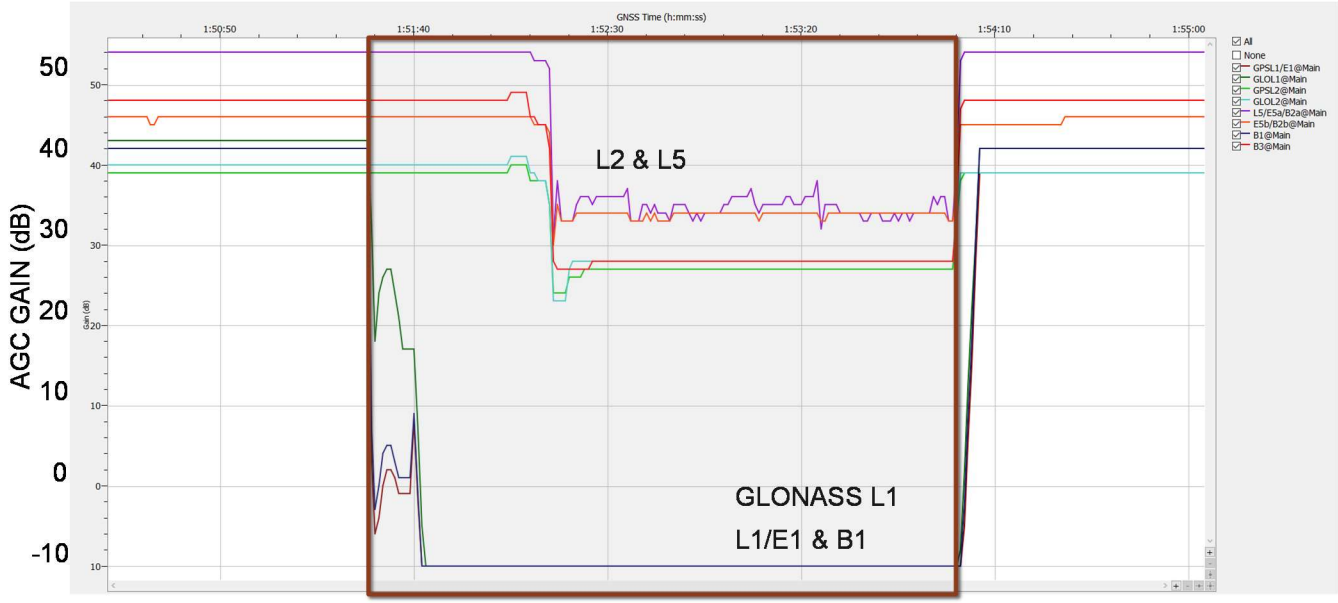

Figure 10. AGC Gain (from Septentrio X5) through ArduSimple ANT2B Antenna during CW Interference Test (Jamming Period highlighted in box)

The increase in noise on these bands is confirmed in the C/No results shown in Figure 11. It shows the C/No on L1 and L2 with L1 practically dropping out a few seconds after jamming starts and L2 having a roughly 15 dB drop about 45 seconds

after the start of jamming (i.e. commensurate to when we see the AGC gain drop). This can also be confirmed when we look at the spectrum plots which are generated from data from the Septentrio re-normalized using the AGC gain level. Figure 12 and Figure 13 show snapshots of the L1 and L2 spectral power levels at different time periods during the test, respectively. From the L1 spectrum shown in Figure 12, one can see the increase in jamming power, especially obvious starting at time 67 seconds (roughly when jamming starts). The two narrowband CW interference signals can be clearly made out as an increase in power around 1575 MHz. Figure 13 shows the L2 spectrum. For the most part, it looks reasonably similar with the maximum power level below -120 dB. However, if we look at time 112 and 165 seconds, the maximum power level increases to about -110 dB and -85 dB, respectively. This corresponds to the periods where the AGC gain drops and near where the transmitted jamming power is at a maximum (see Figure 3). Also, the spectral power distribution is more even (constant) across the band rather the sinusoidal noise power profile across the frequency band for the other time periods. This is further evidence of noise coming into the band at these time periods.

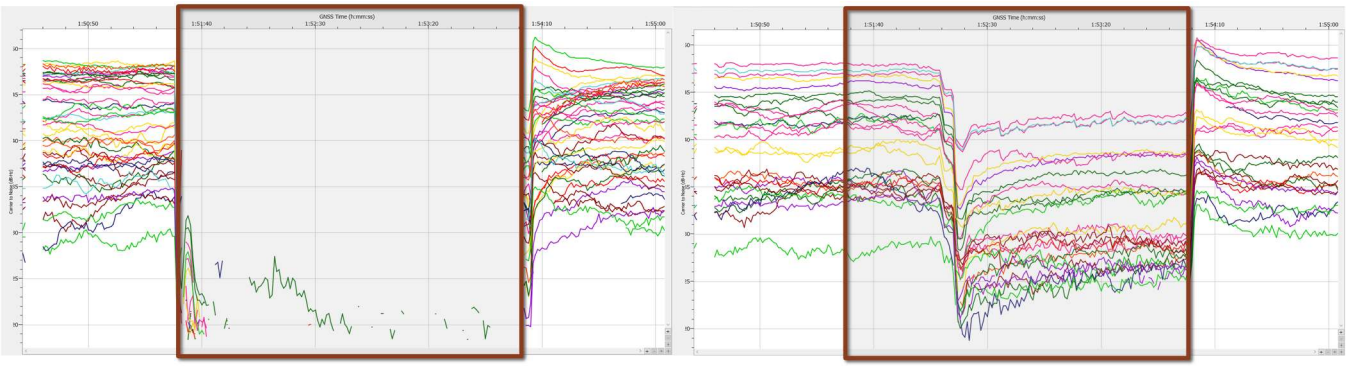

Figure 11. C/No on L1 (Left) and L2 (Right) (from Septentrio X5) through ArduSimple ANT2B Antenna during CW Interference Test (Jamming Period highlighted in box)

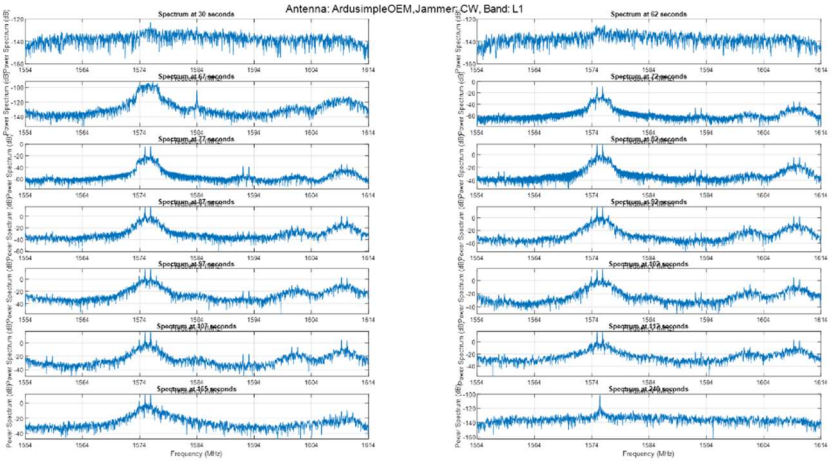

Figure 12. L1 Spectrum (from Septentrio X5, normalized by AGC) through ArduSimple ANT2B Antenna during CW Interference Test

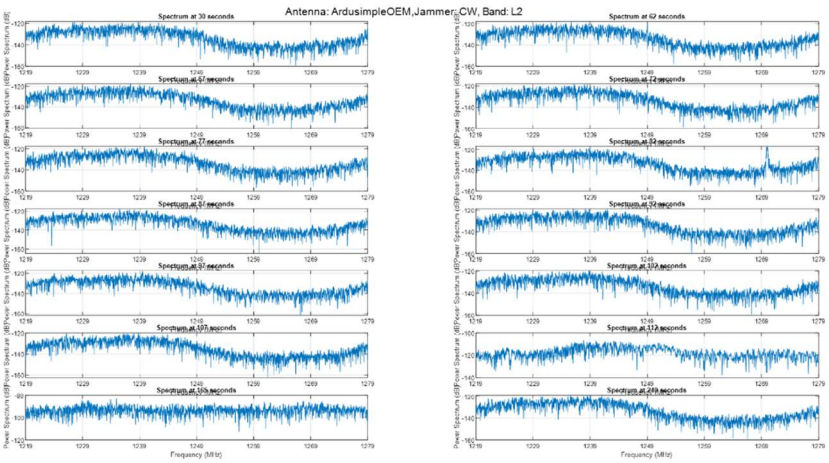

Figure 13. L2 Spectrum (from Septentrio X5, normalized by AGC) through ArduSimple ANT2B Antenna during CW Interference Test

Broadband or Additive White Gaussian Noise (AWGN)

Drastic differences in cross frequency response is not seen with AWGN L1 interference. The Trimble antenna did not show any response or changes in AGC and C/No in the non L1 bands under AWGN L1 interference. The other antennas also did not show any AGC or C/No response in non L1 bands. Figure 14 shows the response of the ArduSimple AGC to L1 interference. The figure shows that the L1 related AGC (L1, E1, B1, GLONASS L1) decreases in a stair step manner rather than a near instantaneous drop AGC in the CW interference case. Even though the AWGN jamming power is the same as the CW jamming, it is much wider band and likely suppressed by the bandpass filters in the antenna and potential receiver filtering. Hence, the actual jamming power seen by the receiver AGC is likely much lower than in the CW jamming case. So, we see a stair step decrease of AGC gain that matches the input jamming power steps. Additionally, the AGC level never reaches its minimum -10 dB value. Indeed, the lowest AGC gain is still 10 dB above the minimum level. Hence the jamming power is not sufficient to max out the AGC and hence unlikely to saturate the LNA. The AGC levels of non-L1 frequency bands do not change in any meaningful way during the L1 AWGN jamming period from its nominal levels. The C/No plots, shown in Figure 15, confirm that there are no cross-frequency effects. The L1 C/No under AWGN interference goes down in the same stair step manner as the AGC gain and the jamming power levels. The L2 C/No does not change noticeably during the interference period.

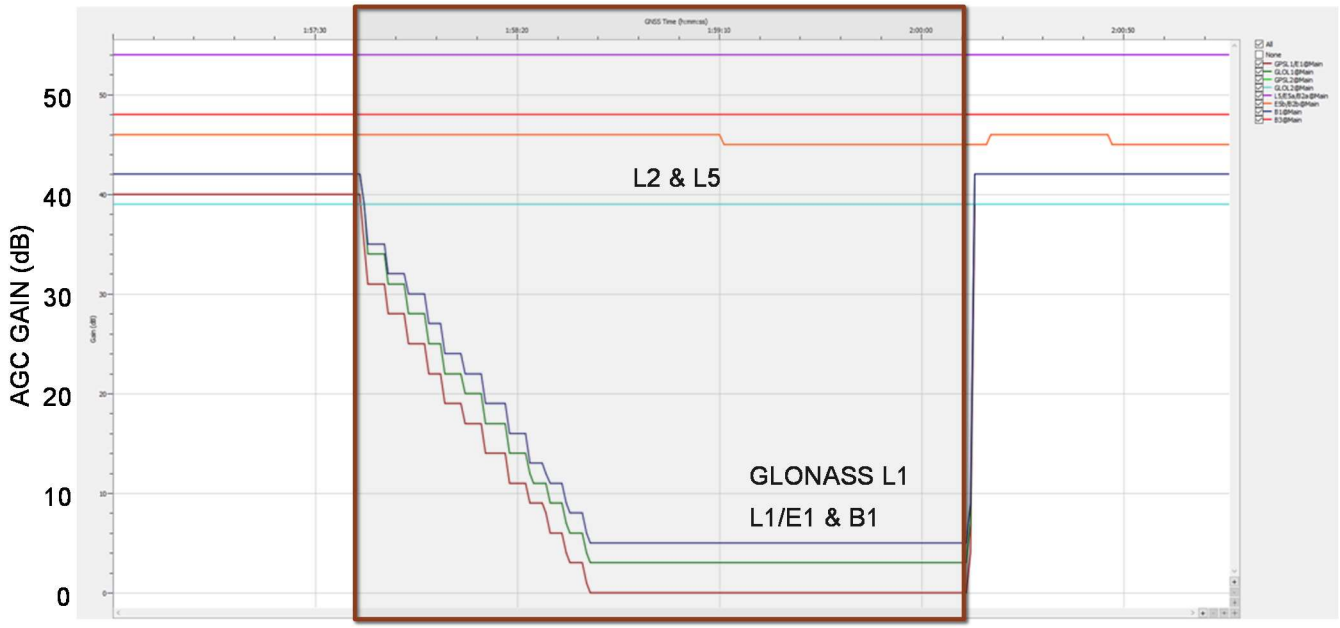

Figure 14. AGC Gain (from Septentrio X5) through ArduSimple ANT2B Antenna during AWGN Interference Test (Jamming Period highlighted in box)

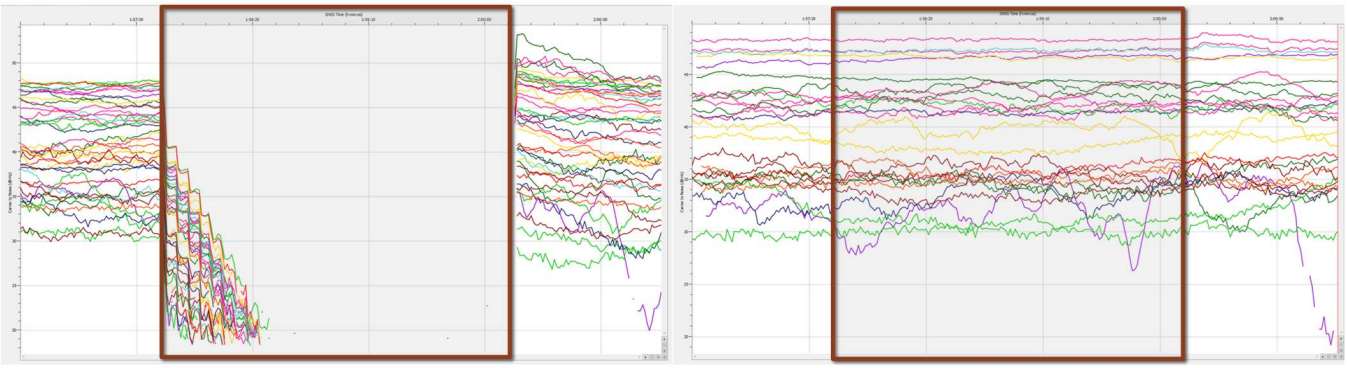

Figure 15. C/No on L1 (Left) and L2 (Right) (from Septentrio X5) through ArduSimple ANT2B Antenna during AWGN Interference Test (Jamming Period highlighted in box)

Figure 16 shows the AGC results from the Trimble Zephyr (Left) and u-blox (Right) under AWGN interference. On both antennas, the AGC indicates that noise level on L1 increases (AGC gain decrease) while the L2 and L5 noise levels remain reasonably constant. The L1 and L2 C/No results, not shown, are similar to that seen in the ArduSimple results. Under this scenario, there is little to no cross-frequency effects. The difference in this interference scenario from the CW is that we are not near the minimum AGC gain level of -10 dB for the Septentrio receiver which we achieved in the CW interference scenario. The lowest AGC level achieved on both the ArduSimple and u-blox are at 0 and 8 dB, respectively which is far from that level. It was only at this minimum level that cross frequency effects were experienced in scenario previously discussed. Hence, it may well be that there is not enough power yet to cause cross frequency effects and suggests that the cause by be due to saturating some component (LNA, etc).

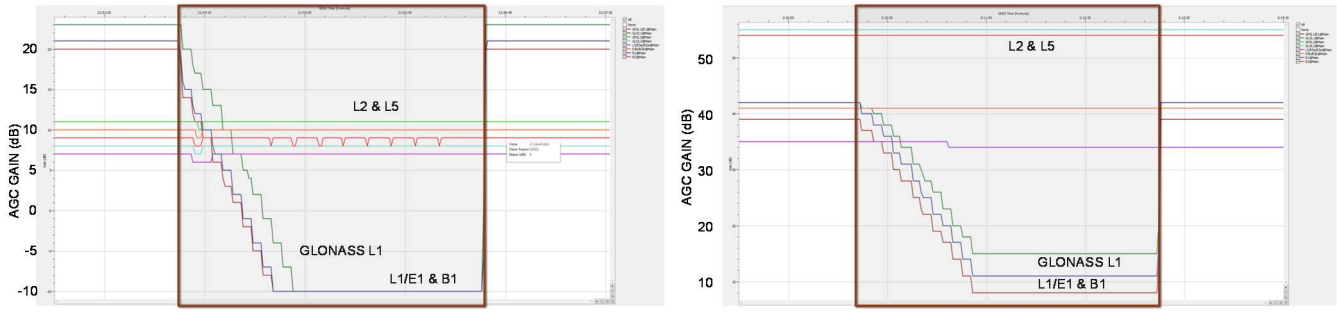

Figure 16. AGC Gain (from Septentrio X5) through Trimble Zephyr (Left) and u-blox ANN-MB1-00 (Right) Antenna during AWGN Interference Test (Jamming Period highlighted in box)

Smartphone Test

Testing receiver effects is ongoing with the first receivers tested being smartphones. In testing smartphones, we examined AGC, C/No and position solution. Spectrum from the receiver antenna is not available as we do not have a direct feed from any of the smartphone antenna. While we tested both forms of interference, the paper will only present the CW interference results. As seen before, this case has more power entering the receiver due to interference power being concentrated near L1. One important thing to note about smartphone AGC is that they are not reported in the same manner. For example, Samsung typically reports a relative AGC level and resets the reference level occasionally (Spens et al, 2021). Fortunately, the test is relatively short and there should not have been a reset. As the smartphone and recording app needs to be turned on, the test data starts off with the phone outside the chamber exposed to the on-air signal (though indoors). Then it is placed inside the chamber and the chamber doors are closed after which it experiences the re-radiated signal.

Continuous Wave Interference (CWI)

Figure 17 shows the L1 (top) and L5 (bottom) AGC gain of the Samsung S20 5G. The initial AGC gain is the value from receiving the on-air signal while outside the chamber. Once in the chamber and subjected to the re-radiated signal, the AGC gain increases by a few dBs. Once the interference is turned on, the L1 AGC gain drops by tens of dBs and is eventually not reported. There is a short period where L1 AGC comes back after being gone (perhaps during an interference power step transition). The L5 AGC is unaffected, at least initially. However, after a while the L5 AGC is no longer reported, presumably due to L5 not being used. Once jamming is turned off, L1 and L5 AGC returns and is at the previous unjammed value. A similar result can be seen in the C/No, shown in Figure 18, where the L1 signal starts to go away during the onset of jamming. L5 stays on with no effect but then suddenly goes away later once no L1 signal is tracked. It is at this point that the receiver also stops providing a position solution. This GNSS seems to show some dependence between L1 and L5 with L5 no longer reporting during part of the L1 jammed interval.

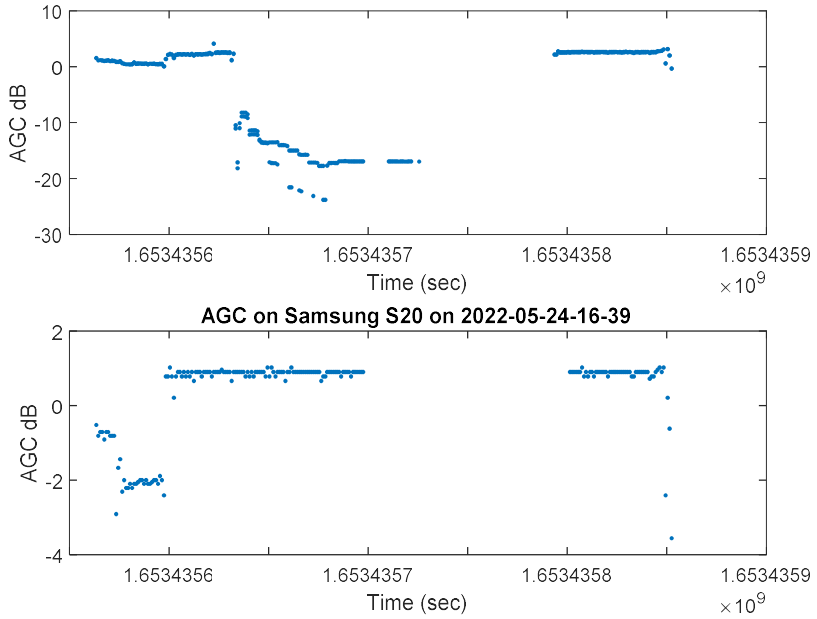

Figure 17. L1 and L5 AGC (Top and Bottom) from Samsung S20 Under CW Interference Test

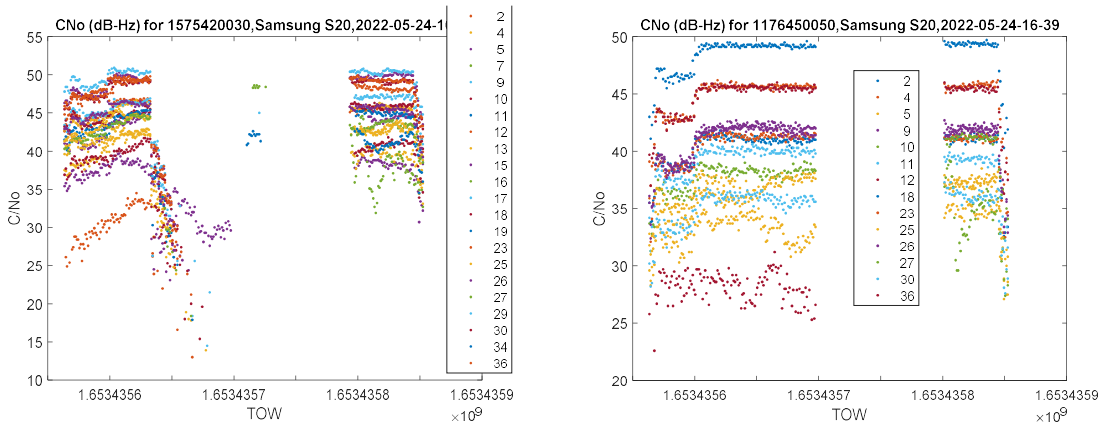

Figure 18. L1 and L5 C/No (Left and Right) from Samsung S20 Under CW Interference Test

Figure 19 shows the L1 and L5 AGC of the Samsung S21 Ultra 5G. The L1 AGC steadily decreases gain while the L5 AGC remains reasonably stable. On first blush, one would expect this to perform similarly to the S20 as it is the same manufacturer, only one year newer, and using a similar top end Snapdragon chipset (865 vs 888 – both 800 series) for that year. However, the figure shows some differences in performance during jamming. In particular, the AGC is reported throughout the jamming indicate that the receiver continues operating. Additionally, the L5 AGC values remain reasonably constant. Figure 20 shows

the C/No on L1 and L5. The L5 C/No showing nearly no signs of L1 interference effects. The one strange, position is not reported throughout the entire jamming period despite having L5. Two possible causes are: 1) L5 positioning requires L1 information (ephemeris) and 2) position is not updated during static operations. While the former is seen in some receivers we have used, the cause is likely the latter as the position reports stop a little before we see C/No jamming effects and resume quite a while after jamming is off. The lack of reporting seems more to correspond to the times between putting on and picking up the phone. While the former (possibility 1) may also be the case, we cannot tell from our current test result.

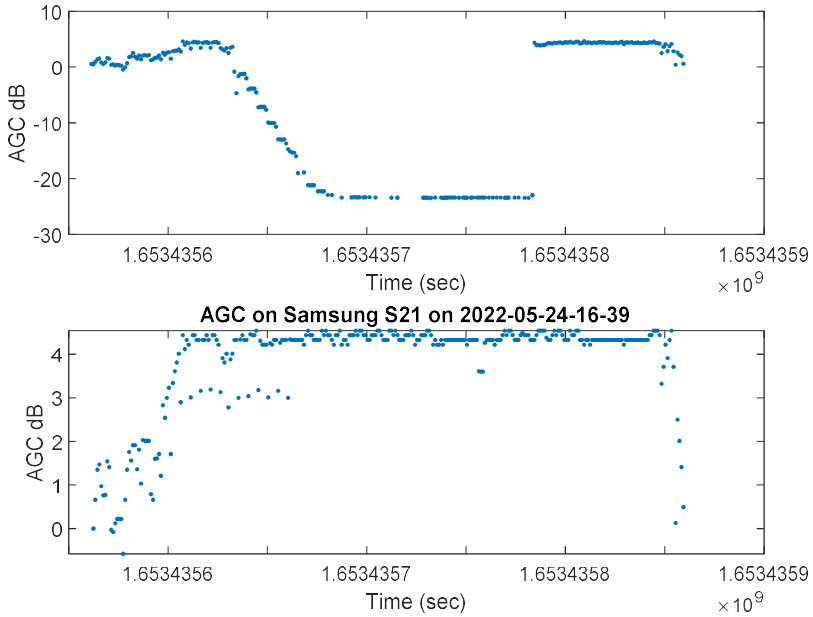

Figure 19. L1 and L5 AGC (Top and Bottom) from Samsung S21 Ultra Under CW Interference Test

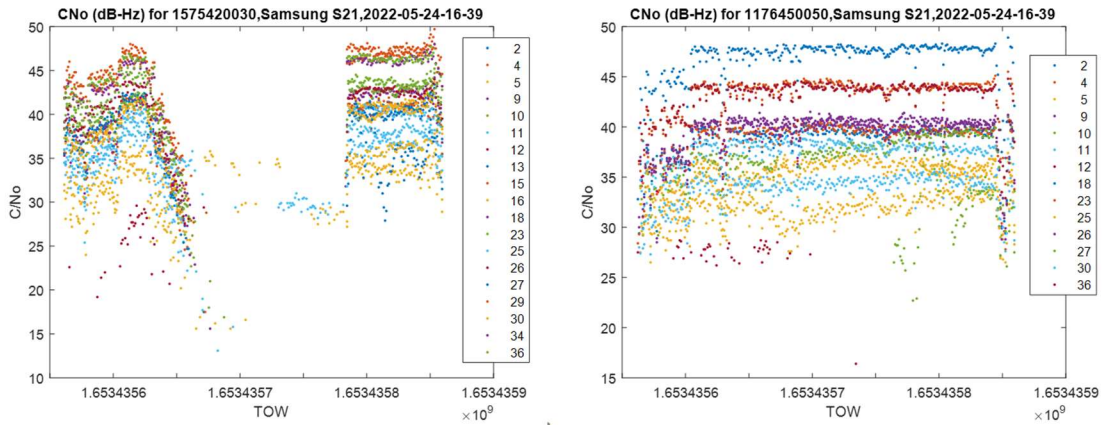

Figure 20. L1 and L5 C/No (Left and Right) from Samsung S21 Under CW Interference Test

Figure 21 shows the AGC results for the Xiaomi Mi 8. The L1 AGC gain decreases to about 18 dB (from about 48 dB) as interference power increases until it jumps to the highest level (around 60 dB) and remains there. Looking at the L1 C/No, there is no noticeable changes or discontinuities in the C/No of tracked signals during this jump which make us suspect that this is the lowest level of AGC gain and the result is an artifact of reporting the AGC. Once jamming is off, the AGC returns to its nominal value from the start. The L5 AGC is unchanged during the entire test though it fluctuates 10 dB, even prior to jamming. Figure 22 shows the C/No on L1 and L5. The C/No results show the effect of jamming as it knocks out tracking of most, but not all signals in the L1 band. Some signals are unaffected and as the Mi 8 is an international phone, this can be any of four satellites systems (GPS, GLONASS, Galileo and Beidou). L5 is generally unaffected though one signal was lost

during the jamming period. The Mi 8 provided a position solution throughout the jamming period hence it is possible that the receiver may be able to operate on L5 only.

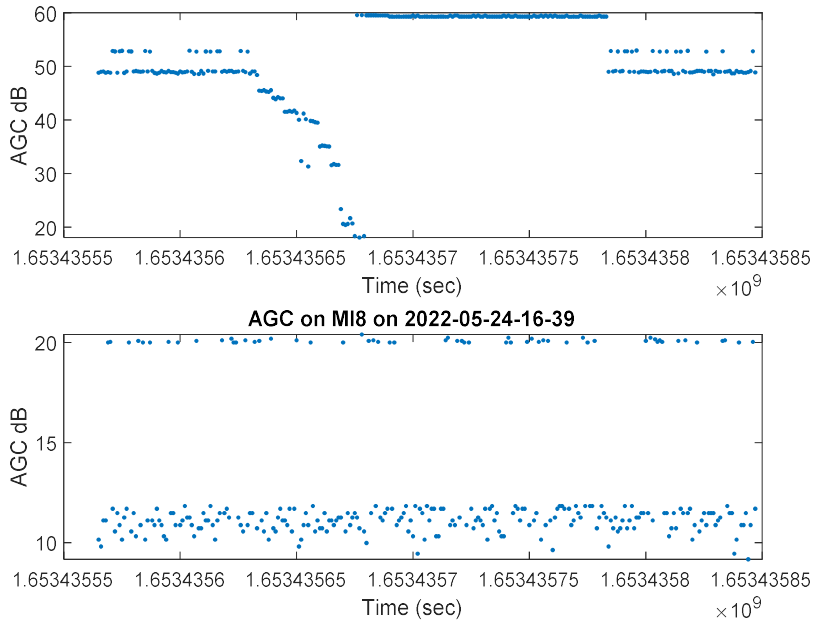

Figure 21. L1 and L5 AGC (Top and Bottom) from Xiaomi Mi 8 Under CW Interference Test

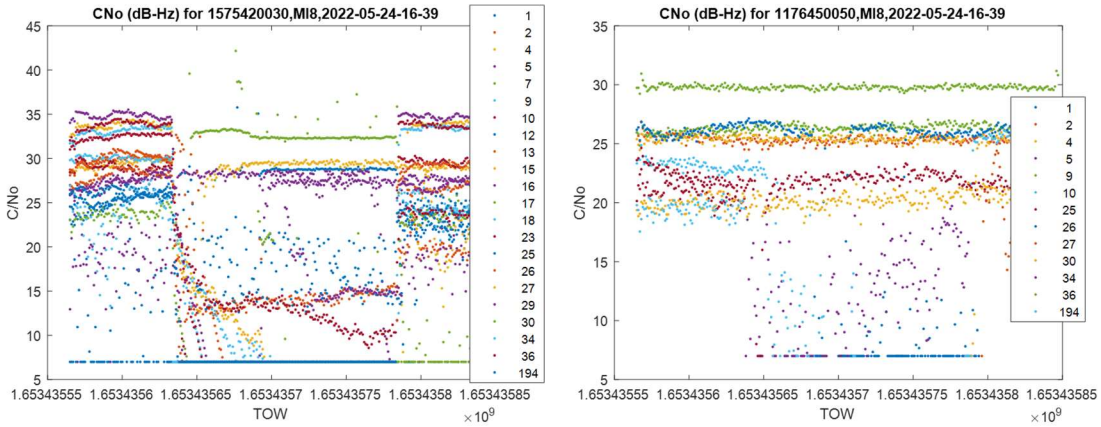

Figure 22. L1 and L5 C/No (Left and Right) from Xiaomi Mi 8 Under CW Interference Test

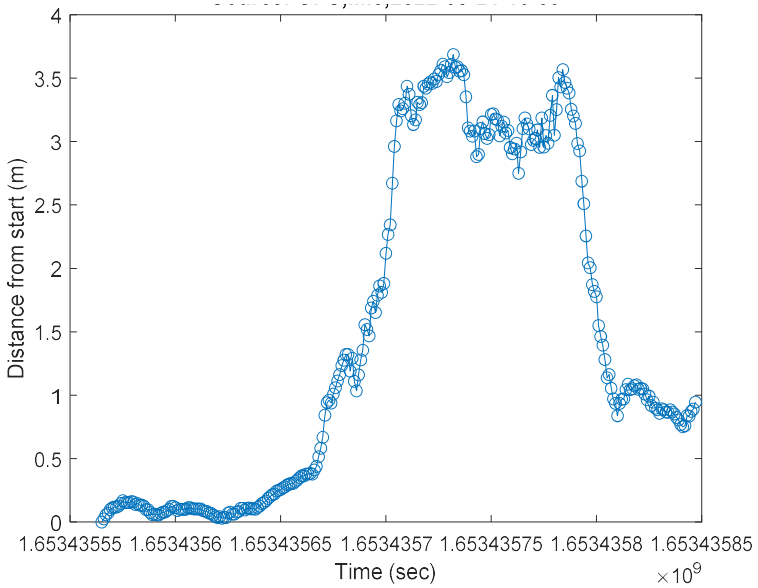

Figure 23. Distance of Current Position from Initial Position from Xiaomi Mi 8 Under CW Interference Test

5. OBSERVATIONS AND SUMMARY

This paper presented cross-frequency effects of interference on GNSS systems. The paper tested antenna and smartphones with on air interference in an anechoic chamber. It showed some examples of antennas or receivers that had nominally independent channels not behaving independently under interference. The antenna used showed different behavior of the same RFI across frequency bands. The survey grade antenna had little cross effects while the other, lower cost, more consumer-oriented, antennas showed some noticeable effects on L2 and L5 band from interference on L1. Tests were conducted with different, recent model smartphones. We tested three different smartphones (Samsung S21 Ultra, Samsung S20, and Xiaomi Mi 8) and found different levels of cross frequency dependence in their signal processing. In one smartphone GNSS (Samsung S20), interference on L1 frequency prevented tracking on L5 while no effect was seen on the other two smartphones

The likely causes of the cross-frequency effects between different antennas are known effects and can be mitigated in many ways. One example is to use amplifiers and mixers that do not go non-linear (or saturate) until higher power levels. These are more expensive and consume more power hungry. The issues seen in the smartphone receivers seem to be processing design issues and are also addressable.

Our work is ongoing and there are still much analyses to conduct – such as examining other receivers and examining interference on other (non-L1) frequencies. For example, on the Samsung S20 smartphone, while interference on L1 affected L5 tracking, interference on L5 did not affect L1 tracking indicating that L1 is used to aid L5 but not vice versa. This work is not meant to be comprehensive – there are many factors. Hopefully this work is to illustrate an issue that critical users of GNSS should be aware of. Hopefully it will get more people examining the issue to understand the effect of implementation on multi-frequency GNSS systems. We then can be better guided by actual performance and not just assume each frequency band will operate independently. This is important for understanding our operational resiliency and to making sure standards for these systems in safety of life applications properly address possible dependencies.

ACKNOWLEDGMENTS

The authors thank the Federal Aviation Administration (FAA) for sponsoring this research. The authors also thank the Logan Scott for his feedback and comments.

The views expressed herein are those of the authors only and are not to be construed as official or those of any other person or organization.

REFERENCES

Amoroso, F, “Overcoming-hard-limiter-suppression,” Microwave Journal, Feb 2003. https://www.microwavejournal.com/articles/3596-overcoming-hard-limiter-suppression

ArduSimple ANT2B Datasheet, https://www.mouser.com/datasheet/2/1042/simpleANT2B_OEM_Datasheet-1917878.pdf

Bastide, F., Akos, D., Macabiau, C., Roturier, B., Automatic Gain Control (AGC) as an Interference Assessment Tool, Proceedings of the 16th International Technical Meeting of the Satellite Division of The Institute of Navigation (ION GPS/GNSS 2003), Portland, OR, September 2003, pp. 2042-2053.

Davenport, Jr., W. B., "Signal-to-noise Ratios in Bandpass Limiters," Journal of Applied Physics , Vol. 24, No. 6, June 1953, pp. 720-727.

Grant, A., Williams, P., Ward, N., & Basker, S. (2009). GPS Jamming and the Impact on Maritime Navigation. Journal of Navigation, 62(2), 173-187. doi:10.1017/S0373463308005213

Lo, S., Enge, P., and Narins, M. (2015), Design of a Passive Ranging System Using Existing Distance Measuring Equipment (DME) Signals & Transmitters. *NAVIGATION*, 62(2), 131– 149. doi: 10.1002/navi.83.

Spens, N., Lee, D.-K., Akos, D. (2021), An Application for Detecting GNSS Jamming and Spoofing, Proceedings of the 34th International Technical Meeting of the Satellite Division of The Institute of Navigation (ION GNSS+ 2021), St. Louis, Missouri, pp. 1981-1988. https://doi.org/10.33012/2021.18027

u-blox ANN-MB1-00 Datasheet, https://www.mouser.com/datasheet/2/1025/ANN_MB1_DataSheet_UBX_21005551-2498077.pdf

WJ Communications, “Mixer Application Information,” The Communications Edge, Tech-note, 2001. https://www.rfcafe.com/references/articles/wj-tech-notes/mixer-application-information.pdf